Journal of Visualized Experiments

Adoptive immunotherapy of iNKT cells in glucose-6-phosphate isomerase (GPI)-induced RA mice
--Manuscript Draft--

Article Type:	Invited Methods Article - JoVE Produced Video
Manuscript Number:	JoVE60048R4
Full Title:	Adoptive immunotherapy of iNKT cells in glucose-6-phosphate isomerase (GPI)-induced RA mice
Section/Category:	JoVE Immunology and Infection
Keywords:	rheumatoid arthritis; adoptive immunotherapy; iNKT cell; cytokines; glucose-6-phosphate isomerase (GPI); in vivo imaging system (IVIS)
Corresponding Author:	Ming Meng Hebei University Baoding, CHINA
Corresponding Author's Institution:	Hebei University
Corresponding Author E-Mail:	mengming127@163.com
Order of Authors:	Ming Meng
	Huifang Liu
	Shengde Chen
	Yuanyuan Wang
	Haiyang Dou
	Wenjuan Li
	Dongzhi Chen
Additional Information:	

Question	Response
Please indicate whether this article will be Standard Access or Open Access.	Standard Access (US$2,400)
Please indicate the **city, state/province, and country** where this article will be **filmed**. Please do not use abbreviations.	Baoding, Hebei Province, China

1   **TITLE:**
2   **Adoptive Immunotherapy of iNKT Cells in Glucose-6-Phosphate Isomerase (G6PI)-Induced RA**
3   **Mice**
4

5   **AUTHORS AND AFFILIATIONS:**
6   Ming Meng[1,2*], Huifang Liu[1,2*], Shengde Chen[1,2*], Yuanyuan Wang[1,2*], Haiyang Dou[1,2*], Wenjuan
7   Li[1,2*], Dongzhi Chen[1,2*]
8
9   [*]These authors contributed equally.
10
11   [1]Medical School of Hebei University, Baoding, Hebei Province, P.R. China
12   [2]Key Laboratory of Pathogenesis Mechanism and Control of Inflammatory-Autoimmune Diseases
13   in Hebei Province, Baoding, P.R. China
14

15   **Corresponding Author:**
16   Dongzhi Chen
17   chenddzz@163.com
18

19   **Email Addresses of Co-authors:**
20   Ming Meng   (mengming127@163.com)
21   Huifang Liu   (liuhuifang93623@163.com)
22   Shengde Chen   (chensd109@163.com)
23   Yuanyuan Wang   (1305271650@qq.com)
24   Haiyang Dou   (douhaiyang-1984@163.com)
25   Wenjuan Li   (lene_li525@163.com)
26

27   **KEYWORDS:**
28   rheumatoid arthritis, adoptive immunotherapy, iNKT cells, cytokines, glucose-6-phosphate
29   isomerase (G6PI), in vivo imaging system (IVIS)
30

31   **SUMMARY:**
32   This protocol uses G6PI mixed peptides to construct rheumatoid arthritis models that are closer
33   to that of human rheumatoid arthritis in CD4^{+} T cells and cytokines. High purity invariant natural
34   killer T cells (mainly iNKT2) with specific phenotypes and functions were obtained by in vivo
35   induction and in vitro purification for adoptive immunotherapy.
36

37   **ABSTRACT:**
38   Rheumatoid arthritis (RA) is a complex chronic inflammatory autoimmune disease. The
39   pathogenesis of the disease is related to invariant natural killer T (iNKT) cells. Patients with active
40   RA present fewer iNKT cells, defective cell function, and excessive polarization of Th1. In this
41   study, an RA animal model was established using a mixture of hGPI325-339 and hGPI469-483
42   peptides. The iNKT cells were obtained by in vivo induction and in vitro purification, followed by
43   infusion into RA mice for adoptive immunotherapy. The in vivo imaging system (IVIS) tracking
44   revealed that iNKT cells were mainly distributed in the spleen and liver. On day 12 after cell

45 therapy, the disease progression slowed down significantly, the clinical symptoms were
46 alleviated, the abundance of iNKT cells in the thymus increased, the proportion of iNKT1 in the
47 thymus decreased, and the levels of TNF-α, IFN-γ, and IL-6 in the serum decreased. Adoptive
48 immunotherapy of iNKT cells restored the balance of immune cells and corrected the excessive
49 inflammation of the body.
50
51 **INTRODUCTION:**
52 Rheumatoid arthritis (RA) is an autoimmune disease characterized by chronic, progressive
53 invasiveness with 0.5–1% incidence[1–2]. The underlying pathogenesis is attributed to the abnormal
54 proliferation of autoreactive CD4^{+} and CD8^{+} T cells, manifested by an increase in the proportion
55 of CD4^{+}IFN-γ^{+} and CD4^{+}IL-17A^{+} T cells, and the reduced number of CD4^{+}IL-4^{+} and
56 CD4^{+}CD25^{+}FoxP3^{+} T cells. Therefore, the secretion of inflammatory cytokines is increased, and an
57 excessive inflammatory reaction destroys the native balance and tolerance function of the body's
58 immune system. Moreover, the helper T lymphocyte (Th) 1 cells that penetrate the joint
59 aggravate the inflammatory response and joint damage. Therefore, the inhibition of excessive
60 inflammatory response and restoration of immune tolerance and immune balance are key to the
61 treatment of RA[3,4].
62
63 The iNKT cells have both NK cell and T cell functions and characteristics. The iNKT cells harbor a
64 distinct, invariant T cell receptor (TCR) α-chain with limited TCR β-chain repertoires[5] and
65 recognize the glycolipid antigen presented by the major histocompatibility complex (MHC) class
66 I molecule CD1d on the surface of the antigen-presenting cells. Mitsuo et al.[6] detected a large
67 number of iNKT cells and functional defects in many autoimmune diseases, including RA. Aurore
68 et al.[7] demonstrated that iNKT cells have a positive effect on maintaining autoimmune tolerance
69 and that when the number and function of iNKT cells are restored, the disease is alleviated. In
70 addition, Miellot-Gafsou et al.[8] found that iNKT cells not only abrogated the disease but also
71 increased the progression of the disease. These contradictory results suggest that iNKT cells are
72 heterogeneous T cells, and the function of different subsets may be reversed. In a clinical study
73 of RA, the frequency of iNKT cells correlated with the score of the disease activity[9]. The results
74 also confirmed that the frequency of iNKT was decreased in RA patients, the number of CD4^{+}IFN-
75 γ^{+} T cell subsets increased, and the secretory levels of inflammatory cytokines IFN-γ and TNF-α
76 increased[10–11]. In addition, Sharif et al.[12] investigated type 1 diabetes (T1D) and found that
77 selective infusion of iNKT cells upregulated the expression of the inflammatory cytokine IL-4,
78 maintained immune tolerance, and prevented the development of type 1 diabetes. Therefore,
79 adoptive infusion of specific iNKT cells or targeted activation of iNKT cells increases the level of
80 iNKT cells in RA patients, which can be a breakthrough in RA treatment.
81
82 Cellular immunotherapy is currently of great interest and has been widely used in cancer therapy.
83 However, iNKT cells are rare, heterogeneous immunoregulatory cells (only 0.3% of the total
84 number of PBMCs)[13], which limits potential clinical applications. These cells are mainly divided
85 into three subpopulations: 1) iNKT1 cells, which have a high expression of promyelocytic
86 leukemia zinc-finger protein (PLZF) and T-box transcription factor (T-bet); 2) iNKT2 cells with
87 intermediate expression of PLZF and GATA binding protein 3 (GATA3); 3) iNKT17 cells with low

88 expression of PLZF and retinoid-related orphan nuclear receptor (ROR)-γt that secrete IFN-γ, IL-
89 4, and IL-17[14]. Activated iNKT cells secrete Th1, Th2, and Th17-like cytokines, which determine
90 the different immunomodulatory effects of iNKT cells[15]. The immunomodulatory and
91 immunotherapeutic effects of specific activation of various subpopulations of iNKT cells are
92 different. Therefore, the selection of specific phenotypes of iNKT cells (mainly iNKT2) with anti-
93 inflammatory functions to regulate the immune response of the body can correct the immune
94 imbalance and immune disorders in RA.
95
96 The establishment of an ideal animal model is of great significance for the treatment and study
97 of RA pathogenesis. Presently, the most commonly used and mature animal models include
98 collagen-induced arthritis, adjuvant arthritis, zymosan-induced arthritis, and polysaccharide-
99 induced arthritis[16–17]. However, there is no model that can fully simulate all the features of
100 human RA. Type II collagen-induced arthritis (CIA) is a classic arthritis model. The CIA is induced
101 by immunization of mice with type II collagen-specific monoclonal antibodies, reflecting the
102 antibody dependence of this disease model. Benurs et al. described a model with a systemic
103 immune response to glucose-6-phosphate isomerase (G6PI), which induces peripheral symmetric
104 polyarthritis in susceptible mouse strains[18,19]. In this model, the development of arthritis depends
105 on T cells, B cells, and innate immunity[18–20]. Horikoshi[21] found that RA models resulting from
106 immunization of DBA/1 mice with G6PI polypeptide fragments are more similar to human RA in
107 terms of CD4^{+} T cells and cytokines (i.e., IL-6 and TNF-α) than the CIA models. In order to increase
108 the stimulating effect on the TCR recognition site, the mixed polypeptide fragments of G6PI
109 (hGPI325-339 and hGPI469-483) were used to immunize DBA/1 mice to construct the RA mouse
110 model. The success rate of this approach can high because hGPI325-339 and hGPI469-483 are
111 immunodominant for I-A q-restricted T cell responses. Therefore, this model can simulate the
112 overproliferation of CD4^{+} T cells and iNKT cell defects in RA patients[22]. The basic research of RA
113 immunopathology laid the foundation for our further in-depth investigation.
114
115 **PROTOCOL:**
116
117 All experimental mice (150 in total) were healthy male DBA/1 mice, 6–8 weeks old (20.0 ± 1.5 g),
118 reared in a specific pathogen-free (SPF) environment. There is no special treatment before
119 modeling. The experiment was divided into a healthy control group (15 mice), a model control
120 group (15 mice), and a cell therapy group (55 mice). This study was approved by the Animal
121 Welfare and Ethical Committee of Hebei University.
122
123 **1.   Constructing the disease model**
124
125 1.1.   Duplicating the RA animal model
126
127 1.1.1.   Weigh 1.75 mg of both hG6PI 325-339 and hG6PI 469-483 fragments and dissolve them
128 in 5.25 mL of 4 °C triple distilled water.
129
130 1.1.2.   Dissolve complete Freund's adjuvant (CFA) in a 50 °C water bath, draw 5.25 mL into

131 another 10 mL centrifuge tube, and cool it for use.

133 1.1.3.   Put the mixture of hG6PI solution and CFA solution in an artificial emulsification unit with
134 two glass syringes connected.

136 1.1.4.   Push the syringe at a constant speed and frequency of 10–20x per min to completely
137 emulsify the mixed peptide solution and CFA solution. Perform the operation in an ice bath, and
138 keep the emulsion droplets in the water for 10 min after the completion of the emulsification
139 without dispersing.

141 1.1.5.   Inject 150 μL of emulsified hG6PIs into the mouse's tail root subcutaneously.

143 1.1.6.   Inject 200 mg of Pertussis toxin into the mouse intraperitoneally at 0 h and 48 h after
144 the hG6PI injection.

146 **1.2.   Experimental verification of the RA model**

148 1.2.1.   Measure the thickness of the mouse's paw with a Vernier caliper (2x a day).

150 1.2.2.   Observe and mark the degree of redness and swelling of the foot. Use the following
151 scoring criteria: 1) toes with mild swelling; 2) dorsum pedis and foot pad with clear red swelling;
152 3) ankle with red swelling.

154 1.2.3.   Euthanize the mice under deep anesthesia by intraperitoneal injection of 1% sodium
155 pentobarbital (50 mg/kg body weight) 14 days after modeling and remove the paws for HE
156 staining.

158 1.2.4.   Determine the secretion levels of serum IL-2, IL-4, IL-6, IL-10, IL-17A, TNF-α, and IFN-γ
159 using a commercial cytometric bead array (CBA) assay according to the manufacturer's
160 protocol.

162 **2.   Obtaining iNKT cells with adoptive cellular therapy**

164 **2.1.   Directional induction of iNKT cells**

166 2.1.1   Inject normal mice intraperitoneally with α-GalCer (0.1 mg/kg of body weight).

168 **2.2.   Isolation of iNKT cells**

170 2.2.1.   Three days after modeling, inject mice intraperitoneally with 1% sodium pentobarbital
171 (50 mg/kg of body weight) for anesthetization. Adequately anesthetized mice do not show a
172 hind paw withdrawal response to a toe pinch.

174   2.2.2.   Isolate the spleen of a DBA/1 mouse after injecting it intraperitoneally with α-GalCer.
175   Prepare a single cell suspension by cutting and grinding the spleen in a 200 mesh sieve.

176

177   2.2.3.   Wash the cell suspension with PBS, centrifuge at 200 x g for 5 min, and discard the
178   supernatant. Repeat.

179

180   2.2.4.   Resuspend the cells with 1 mL of whole blood and tissue dilution solution. Add 3 mL of
181   mouse lymphocyte separation medium, and then centrifuge the cells for 20 min at 300 x g at
182   room temperature.

183

184   2.2.5.   Collect the layer of milky white lymphocytes (i.e., the second layer from the top), wash it
185   2x with PBS, and count with an automated cell counter.

186

187   **2.3.**   **Magnetic activated cell sorting (MACS) positive selection strategy for purification of**
188   **iNKT cells**

189

190   NOTE: For the pretreatment of CD1d tetramers, 1 mg/mL of α-Galcer was diluted to 200 µg/mL
191   with 0.5% of Tween-20 and 0.9% of NaCl, and 5 µL of the resulting solution was added to 100 µL
192   of the CD1d tetramer solution. The mixture was incubated for 12 h at room temperature and
193   placed at 4 °C for use. TCR β was diluted 80x with deionized water. All other antibodies were
194   used as a stock solution.

195

196   2.3.1.   Resuspend 10^7 cells with 100 µL of 4 °C PBS, add 10 µL of α-GalCer-loaded CD1d
197   Tetramer-PE, and incubate them at 4 °C for 15 min in the dark.

198

199   2.3.2.   Wash the cells 2x with PBS and resuspend them in 80 µL of PBS.

200

201   2.3.3.   Add 20 µL of anti-PE-MicroBeads and incubate them at 4 °C for 20 min in the dark.

202

203   2.3.4.   Wash them 2x with PBS and resuspend the cells with 500 µL of PBS.

204

205   2.3.5.   Place the sorting column in the magnetic field of the MACS sorter and rinse with 500 µL
206   of PBS.

207

208   2.3.6.   Add the cell suspension from step 2.3.4 to the sorting column, collect the flowthrough,
209   and rinse 3x with PBS buffer.

210

211   2.3.7.   Remove the magnetic field and collect the cells from the sorting column. At this point,
212   add 1 mL of PBS buffer to the sorting column, and quickly push the plunger at a constant
213   pressure to drive the labeled cells to the collection tube and obtain purified iNKT cells. Count
214   with an automated cell counter.

215

216   **2.4.**   Identification of the iNKT cell phenotype

2.4.1. Take 1 x 10^6 cells from steps 2.2.5 and 2.3.7, respectively, and resuspend them in 50 μL of PBS.

2.4.2. Antibody incubation: Do not add the antibody to the negative control tube, add 0.5 μL of α-GalCer-PE-CD1d Tetramer or 10 μL of FITC-TCR β in the single positive control tube. Add 0.5 μL of α-GalCer-PE-CD1d tetramer and 10 μL of FITC-TCR β in the sample tube. Incubate them at 4 °C for 30 min in the dark.

2.4.3. Wash the cells in PBS and then centrifuge at 200 x g for 5 min.

2.4.4. Discard the supernatant, add 1 mL of Foxp3 Foxation/Permeabilization working solution, and incubate the cells for 45 min at 4 °C in the dark.

2.4.5. Add 1 mL of 1x Permeabilization Buffer working solution and centrifuge the cells at room temperature for 500 x g at room temperature for 5 min.

2.4.6. Discard the supernatant. Add 1 μL of Alexa Fluor 647 mouse Anti-PLZF and 1 μL of PerCP-Cy 5.5 mouse anti-T-bet (or 1 μL of PerCP-Cy 5.5 mouse anti-RORYt) for 30 min at room temperature in the dark.

2.4.7. Add to 2 mL of Permeabilization Buffer working solution for cleaning.

2.4.8. Discard the supernatant, resuspend the cells in 500 μL of PBS, and measure by flow cytometry.

2.5. Functional identification of iNKT cells

2.5.1. Take 3 x 10^6 iNKT cells from step 2.3.7 and resuspend them in 12 well plates with 1.5 mL of RPMI-1640 incomplete medium (i.e., without serum).

2.5.2. Add phorbol ester (PMA, 50 ng/mL) and ionomycin calcium (IO, 1 μg/mL) and place in a CO_2 incubator for 24 h.

2.5.3. Collect the cell supernatant and detect the secretion levels of IL-2, IL-17A, TNF-α, IL-6, IL-4, IFN-γ, and IL-10 using a commercial CBA assay according to the manufacturer's protocol.

2.6. Experimental study on the migration pathway of iNKT cells in RA mice

2.6.1. Dissolve DiR dye (2.5 mg/mL) in DMSO.

2.6.2. Resuspend iNKT cells in 6 well plates with RPMI-1640 incomplete medium. The density is 1 × 10^6 cells/mL.

260

261   2.6.3.   Add DiR (5 μg/mL) solution and incubate in a CO_2 incubator for 25 min.

262

263   2.6.4.   Wash with PBS and resuspend the cells (3×10^6/300 μL) to obtain DiR-labeled iNKT cells
264 (DiR-iNKT).

265

266   2.6.5.   Inject 1% sodium pentobarbital (50 mg/kg body weight) intraperitoneally to anesthetize
267 the mice. Adequately anesthetized mice do not show a hind paw withdrawal to toe pinch. Apply
268 veterinary ointment to the mouse eyes to prevent dryness while under anesthesia for imaging.

269

270   2.6.6.   Inject DiR-iNKT cells 3×10^6 per mouse into the tail vein with the RA model for 8 days.
271 Monitor the iNKT cells in mice postinjection for 0 min, 10 min, 30 min, 60 min, and day 0 (after
272 3 h), 1, 3, 6, 12, 26, 34, 38, and 42 days using a small animal in vivo imaging system (IVIS). The
273 excitation wavelength used was 748 nm, the emission wavelength was 780 nm, and the
274 exposure time was automatic.

275

276   2.6.7.   Place each mouse in a separate cage after each observation and maintain sternal
277 recumbency. Observe until recovery from anesthesia.

278

279 **3.   Evaluation of adoptive immunotherapy of RA mice with iNKT cells**

280

281   3.1.   iNKT cell adoptive immunotherapy for RA mice

282

283   3.1.1.   Inject 3×10^6 cells iNKT cells per mouse through the tail vein. Randomly select 15 mice
284 that were modeled 8 days prior and obtain iNKT cells without DiR labeling from step 2.3.7 by
285 the tail vein infusion.

286

287   3.2.   Evaluate the efficacy of adoptive immunotherapy for iNKT cells.

288

289   3.2.1.   Measure the thickness of the paw of the mouse, quantify the swelling of the ankle joint,
290 and systematically score after the infusion of iNKT cells as described in steps 1.2.1–1.2.2.

291

292   3.2.2.   Observe the inflammatory cell infiltration and joint changes of the mouse joints as
293 described in step 1.2.3.

294

295   3.2.3.   Determine the secretion levels of IL-2, IL-4, IL-6, IL-10, IL-17A, TNF-α, and IFN-γ as
296 described in step 1.2.4.

297

298   3.3.   Determine the frequency of iNKT cells and subsets.

299

300   3.3.1.   Isolate the mouse thymus and prepare a single cell suspension.

301

302   3.3.2.   Separate the lymphocytes with lymphocyte separation fluid.

303

304   3.3.3.   Determine the iNKT cell frequency and subgroup frequency as described in step 2.4.

305

306   3.4.   Statistical analysis

307

308   NOTE: All data are presented as mean ± SD. Values of $P < 0.05$ were considered statistically
309   significant.

310

311   3.4.1.   Use one-factor analysis of variance (ANOVA). If the variance is satisfied, use the LSD test
312   for further comparison.

313

314   3.4.2.   If the variance is not uniform, use the nonparametric test. Use the Kruskal-Wallis H test
315   for further comparison[31].

316

317   **REPRESENTATIVE RESULTS:**
318   The arthritis index score and paw thickness increased after modeling. Compared with the control
319   group, the toes of the RA model group began to show red swelling at 6 days after modeling, with
320   gradual aggravation. At 14 days, the red swelling in the ankle joint peaked, followed by gradual
321   relief. The thickness of the paw changed similarly ($P < 0.05$) (**Figure 1**).

322

323   The inflammatory cell infiltration increased significantly after modeling. The pathological results
324   showed that the infiltration degree of inflammatory cells in the ankle synovial tissue of the RA
325   model mice was different at different stages. Peak inflammation occurred on day 14 post
326   modeling (**Figure 2**).

327

328   Inflammatory cytokines increased and anti-inflammatory cytokines decreased in the serum. In
329   the RA model group, the serum levels of pro-inflammatory cytokines (TNF-α, IFN-γ, and IL-6)
330   significantly increased ($P < 0.05$), while anti-inflammatory cytokines (IL-4 and IL-10) significantly
331   decreased ($P < 0.05$) (**Figure 3**).

332

333   The iNKT cells obtained by in vivo induction and in vitro purification mainly consisted of iNKT2
334   cell subsets, which secrete anti-inflammatory cytokines. Intraperitoneal injection of α-GalCer
335   increased the frequency of iNKT cells in the body, predominantly the iNKT2 subgroup. The
336   frequency of spleen iNKT cells in normal DBA/1 mice was about 2% of the lymphocytes, (iNKT2
337   was about 5%, iNKT1 about 15%, iNKT17 about 10%). Three days after the intraperitoneal
338   injection of α-GalCer, the frequency of iNKT cells was about 6% of the lymphocytes, (iNKT2 was
339   about 82%, iNKT1 about 1.5%, and iNKT17 about 0.5%). After purification by MACS, the purity of
340   iNKT cells was over 85%, of which iNKT2 was about 92%, iNKT1 about 0.4%, and iNKT17 about
341   0.2% (**Figure 4**).

342

343   The harvested iNKT cells secreted more anti-inflammatory cytokines and fewer inflammatory
344   cytokines. The iNKT cells were isolated from the spleens of normal mice and intraperitoneally
345   injected with α-GalCer 3 days after the mouse spleen (α-GalCer group) and the cytokine levels in

346 the cell culture supernatant were examined. Compared with the control group, the inflammatory
347 cytokines (IL-17A, TNF-α, IFN-γ, and IL-6) of the α-GalCer group significantly decreased ($P < 0.05$),
348 and the anti-inflammatory cytokine IL-4 level significantly increased ($P < 0.05$). There was no
349 significant difference in IL-10 ($P > 0.05$). The IFN-γ/IL-4 ratio significantly decreased ($P < 0.05$)
350 (**Figure 5**).

352 IVIS tracing confirmed that DiR-iNKT cells were adoptively infused into RA mice and immediately
353 appeared in the lungs postinjection. Fluorescence was detected in the liver at 10 min and in the
354 spleen at 60 min (**Figure 6A I, 6A II, 6A III**). In the isolated organs, there was no fluorescence in
355 the thymus and inguinal lymph nodes within 1 h. Fluorescence was detected in the lungs at 0
356 min, the fluorescence intensity was the greatest at 10 min, and then gradually weakened. There
357 was weak fluorescence in the liver at 0 min, and then it gradually increased. The fluorescence in
358 the spleen was detected at 30 min and then gradually increased (**Figure 6AIV, 6C**).

360 After the infusion of DiR-iNKT cells into RA mice, fluorescence was mainly concentrated in the
361 liver and spleen (**Figure 6B I, 6B II, 6B III**), but there was no fluorescence in the thymus and
362 inguinal lymph nodes. The spleen and liver had the highest fluorescence intensity on day 1 after
363 cell infusion, but it gradually weakened. On day 34, the surface fluorescence disappeared. On day
364 42, the fluorescence of the isolated organs disappeared. The average fluorescence signal
365 intensity of liver after the cell infusion was higher than that of the spleen (**Figure 6B IV, 6D**).

367 Adoptive infusion of iNKT cells into RA mice can alleviate disease progression and improve clinical
368 symptoms. The iNKT cells improved the clinical symptoms of RA mice after adoptive infusion.
369 Compared with the untreated RA model group, the swelling of the ankle joint was relieved in the
370 cell treatment group, and the scores significantly decreased from day 10 to day 20 postinjection.
371 In the same period in the cell treatment group, inflammatory cell infiltration in the synovial tissue
372 was reduced in comparison to the RA model group (**Figure 2**).

374 The success rates of thymus iNKT cells increased significantly ($P < 0.05$). Compared with the
375 healthy control group, in the RA model group the rates of iNKT cells in the thymus decreased at
376 the progress (day 11), peak (day 14), and recovery (day 20) stages. At peak inflammation, these
377 values were minimal and rebounded in the remission phase. The cell therapy group showed
378 significantly increased rates of iNKT cells at the peak (day 14) and recovery (day 20) stages in
379 comparison with the RA model group ($P < 0.05$) (**Figure 7**).

381 After iNKT cell infusion, the success rate of iNKT1 and iNKT17 in the thymus decreased and iNKT2
382 increased. Compared to the control group, in the RA model group on day 11 iNKT1 and iNKT17 in
383 the thymus significantly increased ($P < 0.05$), and iNKT2 significantly decreased ($P < 0.05$). On day
384 14, iNKT1 and iNKT2 in the thymus significantly increased ($P < 0.05$) and iNKT17 significantly
385 decreased ($P < 0.05$). On day 20, iNKT1 in the thymus significantly increased ($P < 0.05$), iNKT2 did
386 not significantly change ($P > 0.05$), and iNKT17 significantly decreased ($P < 0.05$). The iNKT1/iNKT2
387 ratio significantly increased during all three stages ($P < 0.05$).

389   Compared to the RA model group, on day 11 in the α-GalCer and the cell therapy groups, iNKT1
390   and iNKT17 were significantly lower ($P < 0.05$) and iNKT2 significantly increased ($P < 0.05$). On
391   day 14, in the α-GalCer group iNKT1 and iNKT17 significantly decreased ($P < 0.05$), and iNKT2 did
392   not significantly change ($P > 0.05$); in the cell therapy group iNKT1 and iNKT17 significantly
393   decreased ($P < 0.05$) and iNKT2 significantly increased ($P < 0.05$). On day 20, in the α-GalCer group
394   the iNKT1 significantly decreased ($P < 0.05$), iNKT2 did not change significantly ($P > 0.05$), and
395   iNKT17 significantly increased ($P < 0.05$); in the cell therapy group iNKT1 and iNKT17 significantly
396   decreased ($P < 0.05$) and iNKT2 significantly increased ($P < 0.05$). The ratio of iNKT1/iNKT2
397   significantly decreased during all three stages ($P < 0.05$) (**Figure 7**).
398
399   The levels of inflammatory cytokines were increased in serum and the anti-inflammatory
400   cytokines were decreased after iNKT cell infusion. In the RA model group, the levels of TNF-α,
401   IFN-γ, and IL-6in serum significantly increased (*P < 0.05*), while IL-4 and IL-10 showed markedly
402   decreased amounts (*P < 0.05*) in comparison with the control group. In the iNKT cell therapy
403   group, the levels of TNF-α, IFN-γ, and IL-6 in serum significantly decreased at the progress and
404   peak stages of inflammation (*P < 0.05*), while IL-4 and IL-10 significantly increased (*P < 0.05*) in
405   comparison with the RA model group (**Figure 3**).
406
407   **FIGURE AND TABLE LEGENDS:**
408   **Figure 1. The joint swelling score and paw thickness change in mice.** (**A**) Swelling of the ankle
409   joint in mice. (**B,D**) Paw thickness in different groups. (**C**) Clinical score changes in different
410   groups. The mouse arthritis score and the thickness of the paw were significantly reduced in the
411   cell therapy group on days 10–20 (i.e., 2–12 days after treatment) after modeling. **P < 0.05* vs.
412   control, ***P < 0.05* vs. RA.

413
414   **Figure 2. Histopathological changes of the ankle joint.** The infiltration of inflammatory cells was
415   significantly reduced in the cell therapy group and was significantly increased in the RA group on
416   day 14. ◊ = inflammatory cells. (**A**) 100x (**B**) 400x.
417
418   **Figure 3. The levels of serum cytokines in each group**. (**A**) Serum cytokines levels in mice on day
419   11 after modeling (pg/mL). (**B**) Serum cytokines levels in mice on day 14 after modeling (pg/mL).
420   The levels of TNF-α, IFN-γ, and IL-6 significantly decreased, and the levels of IL-4 and IL-10
421   significantly increased in the cell therapy group. [a]*P < 0.05* vs. control. [b]*P < 0.05* vs. RA.

422
423   **Figure 4. The rates of iNKT cells and proportion of iNKT cell subsets.** (**A,B,C**) The rate of iNKT2 in
424   normal mice is ~5%. (**D,E,F**) The rate of iNKT2 is about 82% after in vivo induction. (**G, H, I**) The
425   rate of iNKT2 is more than 92% after MACS purification.
426
427   **Figure 5. Cytokine levels in culture supernatant of mouse spleen-derived iNKT cells**. The level
428   of IL-4 significantly increased, and the levels of IL-17A, TNF-α, IFN-γ, and IL-6 significantly
429   decreased. [a]*P < 0.05* vs. control.
430

Figure 6. Distribution and metabolism of iNKT cells traced by caliper IVIS lumina II. (**A**,**B**) Migration path of iNKT cells. (**C**) The change of the average fluorescence signal intensity in the spleen, liver, and lung. (**D**) The change of the average fluorescence signal intensity in the spleen and liver. The fluorescence was detected in the lungs and liver at 0 min, and then gradually increased. The fluorescence intensity was strongest at 10 min in the lungs and then decreased. The fluorescence of the spleen was detected at 30 min, then gradually increased. The fluorescence of all organs disappeared on day 42. The average fluorescence signal intensity of the liver is higher than the spleen after cell infusion (I: supine; II: lateral lying; III: prone; IV: isolated tissue; a: control group; b: cell infusion group; 1, 2, 3, 4, 5 are thymus, spleen, liver, inguinal lymph nodes, lungs).

Figure 7. The rates of iNKT and its subsets in the mouse thymus. (**A**) The rates of iNKT cells at 11, 14, and 20 days after modeling. (**B**) The ratio of iNKT1/iNKT2. (**C,D,E**) The rate of iNKT1, iNKT2, and iNKT17. On days 11, 14, and 20 (days 3, 6, and 12 after cell therapy), the rates of iNKT cells significantly increased, the iNKT1 and iNKT17 of the thymus significantly decreased in the cell therapy group, and iNKT2 was significantly increased. [a]$P < 0.05$ vs Control. [b]$P < 0.05$ vs RA.

DISCUSSION:

iNKT cells are special T cells that bridge innate and adaptive immunity and are mainly developed from CD4^{++}/CD8^{+} thymocytes. iNKT cells have diverse immunoregulatory functions and interact with other immune cells by direct contact and secretion of different cytokines[23], affecting dendritic cells (DCs), macrophages, neutrophils, B cells, T cells, and NK cell differentiation and development[24]. α-GalCer is a classical iNKT cell-specific activator extracted from sponges. Several studies indicate that spleen iNKT cell frequency reaches a peak after a single intraperitoneal injection of α-GalCer for 3 days[25]. Our experimental results demonstrated the predominance of the iNKT2 subset in mice spleen for 3 days after an intraperitoneal injection of α-GalCer, which mainly secretes anti-inflammatory cytokines IL-4 and IL-10. We also found that the abundance of iNKT2 cells decreased and that of iNKT1 and iNKT17 cells increased in the RA model mice during the inflammatory phase. Therefore, we isolated the iNKT cells of the mouse spleen by intraperitoneal injection of α-GalCer for 3 days. These were used to treat the RA model mice. The rate of the iNKT2 subset was 82% after in vivo induction. After purification by MACS, the rate of iNKT2 exceeded 92%.

The specific activation of iNKT cells is employed as a novel biological treatment for RA. Horikoshi et al.[21] demonstrated that intradermal injection of α-GalCer inhibited GPI peptide-induced arthritis by significantly inhibiting the number of CD4^{+} T cells. Chiba et al.[26] showed that repeated injections of the synthetic iNKT2 selective activator OCH inhibited CIA, while α-GalCer showed a slight inhibitory effect. We injected spleen-derived iNKT into RA model mice, and the results showed that the degree of swelling of the ankle joints in the cell therapy group and the number of inflammatory cells infiltrating into the joints was reduced. The level of serum anti-inflammatory cytokines (e.g., IL-4 and IL-10) increased, and the secretion of pro-inflammatory cytokines (e.g., IFN-γ and TNF-α) decreased. the targeted activation of iNKT cells was able to alleviate the progression of RA and inhibit the inflammatory response. In addition, we detected

474   the frequency of iNKT in the thymus and found that the number of iNKT cells in the RA model
475   group was significantly reduced, while the frequency in the thymus increased after infusion of
476   the iNKT cells. Due to the presence of the blood-thymus barrier system, we did not consider the
477   adoptively infused increase in the level of iNKT in the thymus that was confirmed in later
478   experiments. Further detection of the subpopulations of iNKT cells in the thymus revealed that,
479   compared to the healthy control group, the number of iNKT1 cells in the RA model group
480   increased significantly during the three stages of inflammation and maximally during the peak of
481   inflammation, while the proportion of the iNKT2 subset began to increase at the peak of
482   inflammation. Notably, the iNKT1 subset might be involved in the early inflammation of RA, and
483   the iNKT2 subset may play an important role in inhibiting the inflammation. Compared to the RA
484   model group, the iNKT1 subset in the cell therapy group significantly decreased during the
485   inflammatory phase, and the iNKT2 subset significantly increased in the early and remission stage
486   of inflammation. These results indicated that adoptive infusion of specific phenotypes and
487   functional iNKT cells significantly increased the frequency of iNKT cells in RA and altered the
488   proportion of iNKT cell subsets.

490   We used IVIS to observe the distribution of iNKT cells in mice after adoptive infusion and found
491   the highest fluorescence intensity in the lungs 10 min after infusion, which faded gradually. The
492   liver showed weak fluorescence, which increased gradually and decreased gradually after 2 days.
493   Fluorescence was detected in the spleen at 30 min, which increased gradually and decreased
494   after 2 days. The average fluorescence intensity of the liver was stronger than that of the spleen.
495   However, no fluorescence was detected in the thymus and inguinal lymph nodes. The detection
496   of fluorescence in the lungs might be attributed to the infusion of iNKT cells into the tail vein.
497   These cells are circulated to the lungs with the blood. The liver fluoresces earlier than the spleen,
498   and the average fluorescence intensity of the liver is stronger than that of the spleen. This
499   preferential accumulation of the iNKT cells may be due to the abundant blood vessels in the liver,
500   the main metabolic organ. Fluorescence was not detected in the thymus. This might be due to
501   the hematological barrier, which could hinder the entry of iNKT cells. Fluorescence was never
502   detected in the inguinal lymph nodes, perhaps because fewer iNKT cells entered the lymph nodes
503   and did not reach the minimum level of detection. Also, it could be speculated that the iNKT cells
504   infused into the tail vein might not enter the lymph nodes. Therefore, we hypothesize that the
505   development and differentiation of iNKT cells in the thymus might be regulated through cytokine
506   pathways after adoptive infusion into the mice. This needs to be elucidated further.

508   GPI is present in the serum and synovial fluid of most RA patients and is a commonly used test
509   for clinical RA diagnosis[27]. Bruns et al.[28] used peptides of different lengths from the GPI sequence
510   and immunized the DBA/1 mice to identify six immunodominant T cell epitopes. Of these, three
511   were arthritogenic. The peptides with >95% incidence of arthritis are hGPI 325-339 and hGPI469-
512   483. Our previous studies demonstrated that the use of a mixture of the two peptides to establish
513   an RA model is better than a single peptide. In the resulting RA models, the toes and joints of the
514   mice began to appear red on day 6 and reached a peak of inflammation on day 14. The
515   inflammatory cell infiltration was accompanied by tissue hyperplasia in the synovial tissue of the
516   joints, and the inflammatory cell infiltration was most severe at day 14. The number of iNKT cells

517 was decreased significantly in the thymus at the peak of inflammation, which was consistent with
518 the trend of iNKT cells in RA patients[29]. Further detection of iNKT cell subsets revealed that the
519 frequency of iNKT1 and iNKT17 in the thymus increased and the frequency of iNKT2 decreased
520 during the progression of inflammation (day 11). In addition, the levels of serum cytokines IFN-γ
521 and IL-17A increased during the progression (day 11) and the peak of inflammation (day 14),
522 suggesting a similar polarization of the Th1 and Th17 subgroups in RA model mice[30]. Therefore,
523 the RA mouse model induced by hGPI325-339 and hGPI469-483 mixed polypeptide fragments
524 exhibited the characteristics of CD4$^+$ T cell hyperproliferation and iNKT cell defects, which was
525 similar to that of the RA patients, and could be used as an ideal animal model for investigating
526 the immunity of the RA cells. These results were in agreement with those from our previous
527 studies and demonstrated the stability of the hGPIs-induced RA model[31].
528
529 In general, the RA mouse model induced by the mixed G6PI peptides can simulate the changes in
530 CD4$^+$ T cells, iNKT cells, and related cytokines in RA patients. This provides a good model for in-
531 depth investigation of RA. Consequently, iNKT (mainly iNKT2) induced by intraperitoneal
532 injection of α-GalCer and purified in vitro was used in the treatment of RA. It can correct the
533 immune imbalance caused by abnormal proliferation of Th subsets, relieve the progression of
534 RA, and in the future may provide novel methods for the clinical treatment of RA.
535

542 **DISCLOSURES:**
543 The authors declare no funding or conflicts of interest.
544

545 **REFERENCES:**
546 1.   Tobón, G. J, Youinou, P, Saraux, A. The environment, geo-epidemiology, and autoimmune
547 disease: Rheumatoid arthritis. *Autoimmunity Reviews*. **35** (1), 0–14 (2010).
548 2.   Cross, M. et al. The global burden of rheumatoid arthritis: estimates from the Global
549 Burden of Disease 2010 study. *Annals of the Rheumatic Diseases*. **73** (7), 1316–1322 (2014).
550 3.   Kanashiro, A., Bassi, G. S., Queiróz Cunha, F. D., Ulloa, L. From neuroimunomodulation to
551 bioelectronic treatment of rheumatoid arthritis. *Bioelectronics in Medicine*. **1** (2), 151–165 (2018).
552 4.   Brennan, P.J., Brigl, M., Brenner, M.B. Invariant natural killer T cells: an innate activation
553 scheme linked to diverse effector functions. *Nature Reviews Immunology*. **13** (2), 101–117 (2013).
554 5.   Bianca, B. S. Unraveling Natural Killer T-Cells Development. *Frontiers in Immunology*. **8**,
555 1950 (2018).
556 6.   Mitsuo, A. et al. Decreased CD161+CD8+ T cells in the peripheral blood of patients
557 suffering from rheumatic diseases. *Rheumatology*. **45** (12), 1477–1484 (2006).
558 7.   Miellot, A. et al. Activation of invariant NK T cells protects against experimental
559 rheumatoid arthritis by an IL-10-dependent pathway. *European Journal of Immunology*. **35** (12),

560 3704–3713 (2005).

8. Miellot-Gafsou, A. et al. Early activation of invariant natural killer T cells in a rheumatoid arthritis model and application to disease treatment. *Immunology*. **130** (2), 296–306 (2010).

9. Tudhope, S. J., Delwig, A. V., Falconer, J., Pratt, A., Ng, W. F. Profound invariant natural killer t-cell deficiency in inflammatory arthritis. *Annals of the Rheumatic Diseases*. **69** (10), 1873–1879 (2010).

10. Ming, M. et al. Effects on immunoregulation of iNKT cells in RA by novel synthetic immunostimulator CH1b. *Chinese Journal of Immunology*. **32** (02), 218–222 (2016).

11. Ming, M. et al. Study of the correlation between the percentage of iNKT cells and the ratio of IFN-γ/IL-4 in patients with rheumatoid arthritis. *Chinese Journal of Microbiology Immunology*. **35** (3), 213—218 (2015).

12. Sharif, S. et al. Activation of natural killer T cells by α-galactosylceramide treatment prevents the onset and recurrence of autoimmune Type 1 diabetes. *Nature Medicine*. **7**, 1057–1062 (2010).

13. Gapin, L. Development of invariant natural killer T cells. *Current Opinion in Immunology*. **39**, 68–74 (2016).

14. Kwon, D. I., Lee, Y. J. Lineage Differentiation Program of Invariant Natural Killer T Cells. *Immune Network*. **17** (6) (2017).

15. Thapa, P. et al. The differentiation of ROR-γt expressing iNKT17 cells is orchestrated by Runx1. *Scientific Reports*. **7** (1), 7018 (2017).

16. Schurgers, E., Billiau, A., Matthys, P. Collagen-induced arthritis as an animal model for rheumatoid arthritis: focuson interferon-γ. *Interferon Cytokine Research*. **31** (12), 917–926 (2011).

17. Van Haalen, H. G. M., Severens, J. L., Tran-Duy, A., Boonen, A. How to select the right cost-effectiveness model: A systematic review and stepwise approach for selecting a transferable health economic evaluation model for rheumatoid arthritis. *Pharmacoeconomics*. **32** (5), 429–442 (2014).

18. Schubert, D., Maier, B., Morawietz, L., Krenn, V., Kamradt, T. Immunization with glucose-6-phosphate isomerase induces T cell-dependent peripheral polyarthritis in genetically unaltered mice. *Journal of Immunology*. **172**, 4503–4509 (2004).

19. Bockermann, R., Schubert, D., Kamradt, T., Holmdahl, R. Induction of a B-cell-dependent chronic arthritis with glucose-6-phosphate isomerase. *Arthritis Research & Therapy*. **7**, R131613–24 (2005).

20. Kamradt, T., Schubert, D. The role and clinical implications of G6PI in experimental models of rheumatoid arthritis. *Arthritis Research & Therapy*. **7**, 20-28 (2005).

21. Horikoshi, M. et al. Activation of Invariant NKT Cells with Glycolipid Ligand α-Galactosylceramide Ameliorates Glucose-6-Phosphate Isomerase Peptide-Induced Arthritis. *PlosOne*. **7** (12), e51215 (2012).

22. Zhang, X.-J. et al. Immunization with mixed peptides derived from glucose-6-phosphate isomerase induces rheumatoid arthritis in DBA /1 mice. *Chinese Journal of Pathophysiology*. **32** (3), 569–576 (2016).

23. Motohashi, S., Nakayama, T. Invariant natural killer T cell-based immunotherapy for cancer. *Immunotherapy*. **1** (1), 73 (2017).

24. Jung, S. et al. The requirement of natural killer T-cells in tolerogenic APCs-mediated

603   suppression of collagen-induced arthritis. *Experimental and Molecular Medicine*. **42** (8), 547–554
604   (2010).

605   25.   Luc, V. K., Lan, W. Therapeutic Potential of Invariant Natural Killer T Cells in Autoimmunity.
606   *Frontiers in Immunology*. **9**, 519–526 (2018).

607   26.   Chiba, A. et al. Suppression of collagen-induced arthritis by natural killer T cell activation
608   with OCH, a sphingosine-truncated analog of α-galactosylceramide. *Arthritis & Rheumatism*. **50**
609   (1), 305–313 (2004).

610   27.   Tudhope, S. J., Delwig, A. V., Falconer, J., Pratt, A., Ng, W. F. Profound invariant natural
611   killer t-cell deficiency in inflammatory arthritis. *Annals of the Rheumatic Diseases*. **69** (10), 1873–
612   1879 (2010).

613   28.   Bruns, L. et al. Immunization with an immunodominant self-peptide derived from glucose-
614   6-phosphate isomerase induces arthritis in DBA/1 mice. *Arthritis Research & Therapy*. **11** (4)
615   (2009).

616   29.   Parietti, V. et al. Rituximab treatment overcomes reduction of regulatory iNKT cells in
617   patients with rheumatoid arthritis. *Clinical Immunology*. **134** (3), 331–339 (2010).

618   30.   Yoshida, Y. et al. Functional mechanism(s) of the inhibition of disease progression by
619   combination treatment with fingolimod plus pathogenic antigen in a glucose-6-phosphate
620   isomerase peptide-induced arthritis mouse model. *Biological & Pharmaceutical Bulletin*. **38** (8),
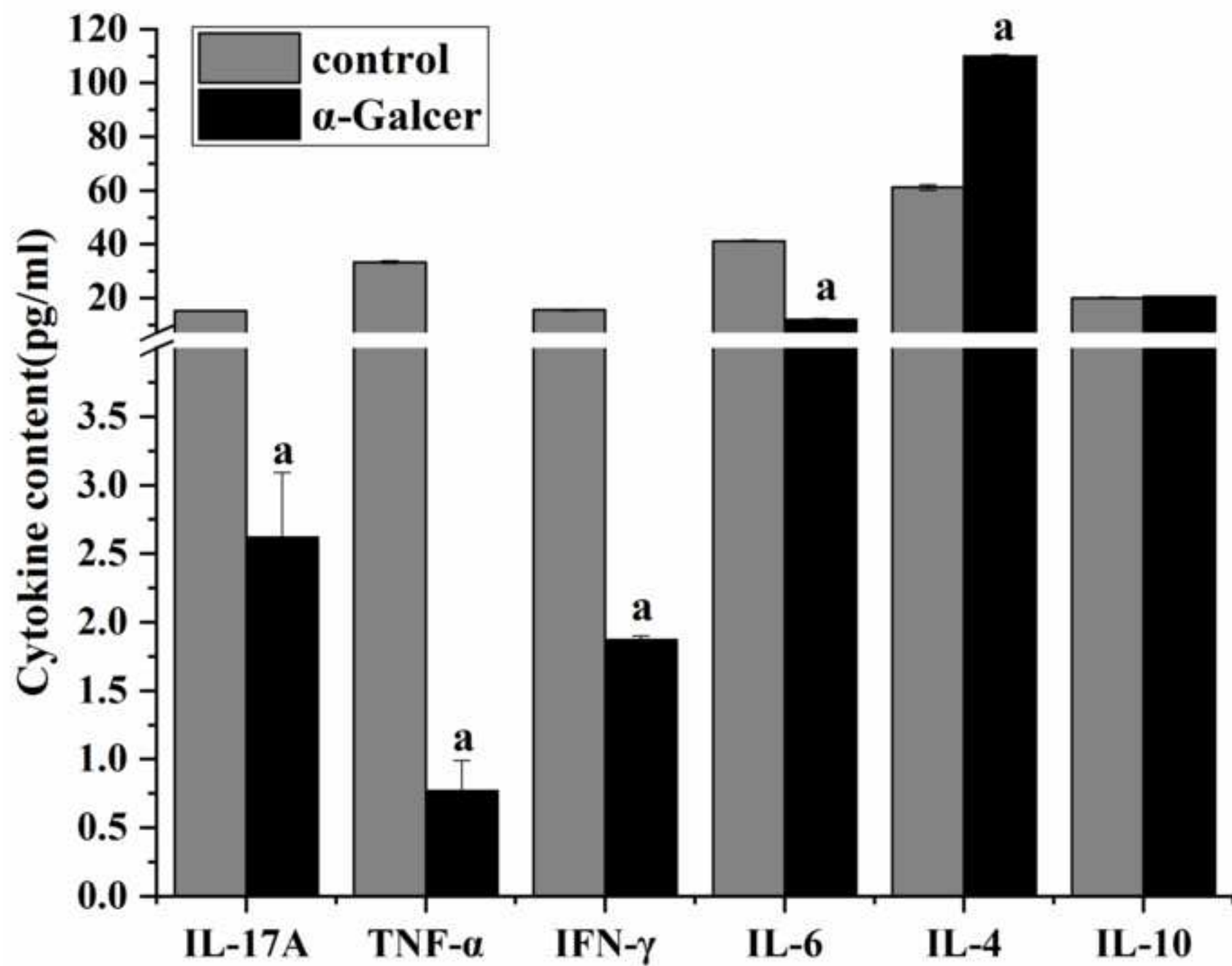621   1120–1125 (2015).

622   31.   Chen, D. et al. Study of the adoptive immunotherapy on rheumatoid arthritis with
623   Thymus-derived invariant natural killer T cells. *International Immunopharmacology*. **67**, 427–440
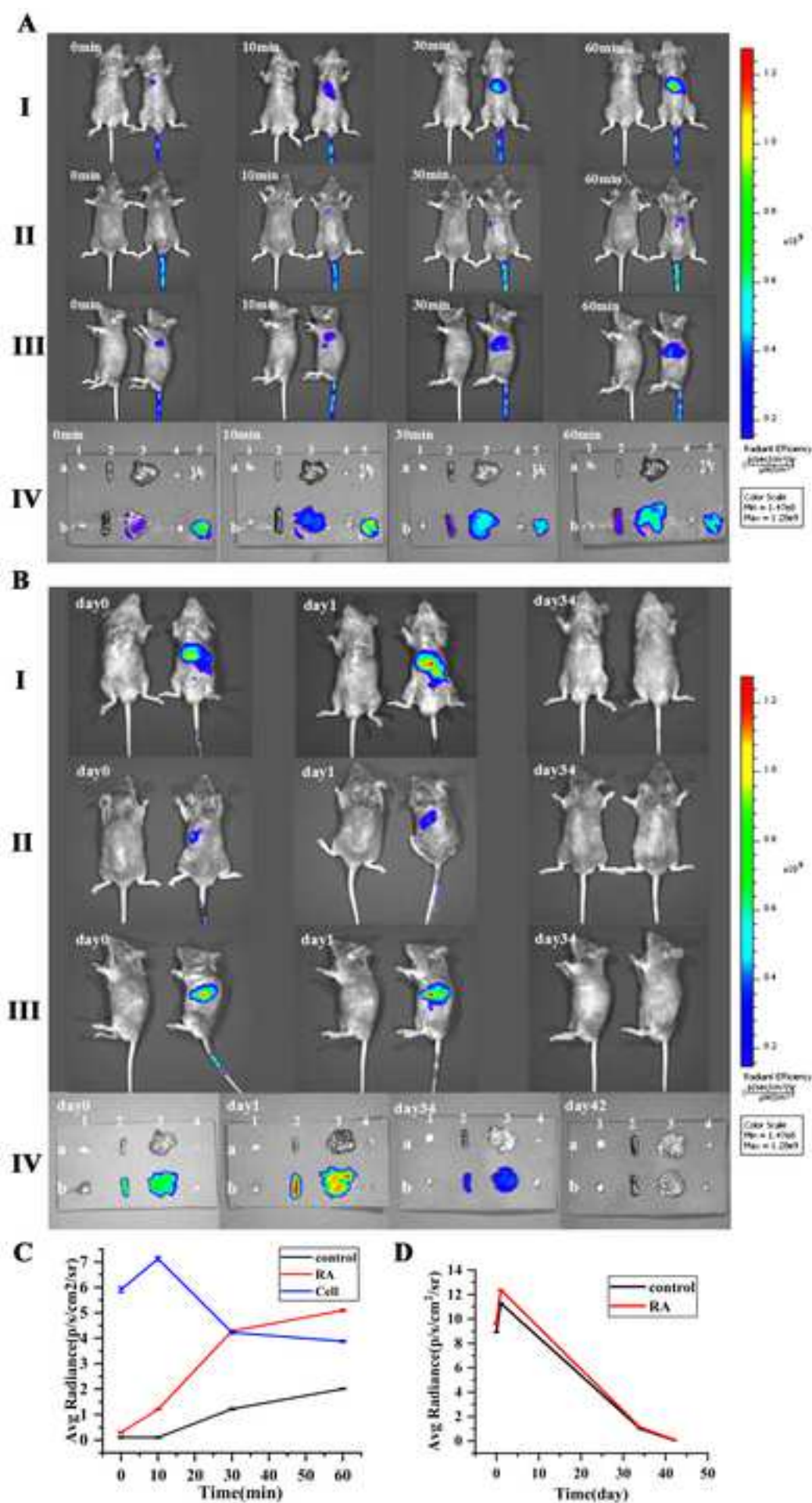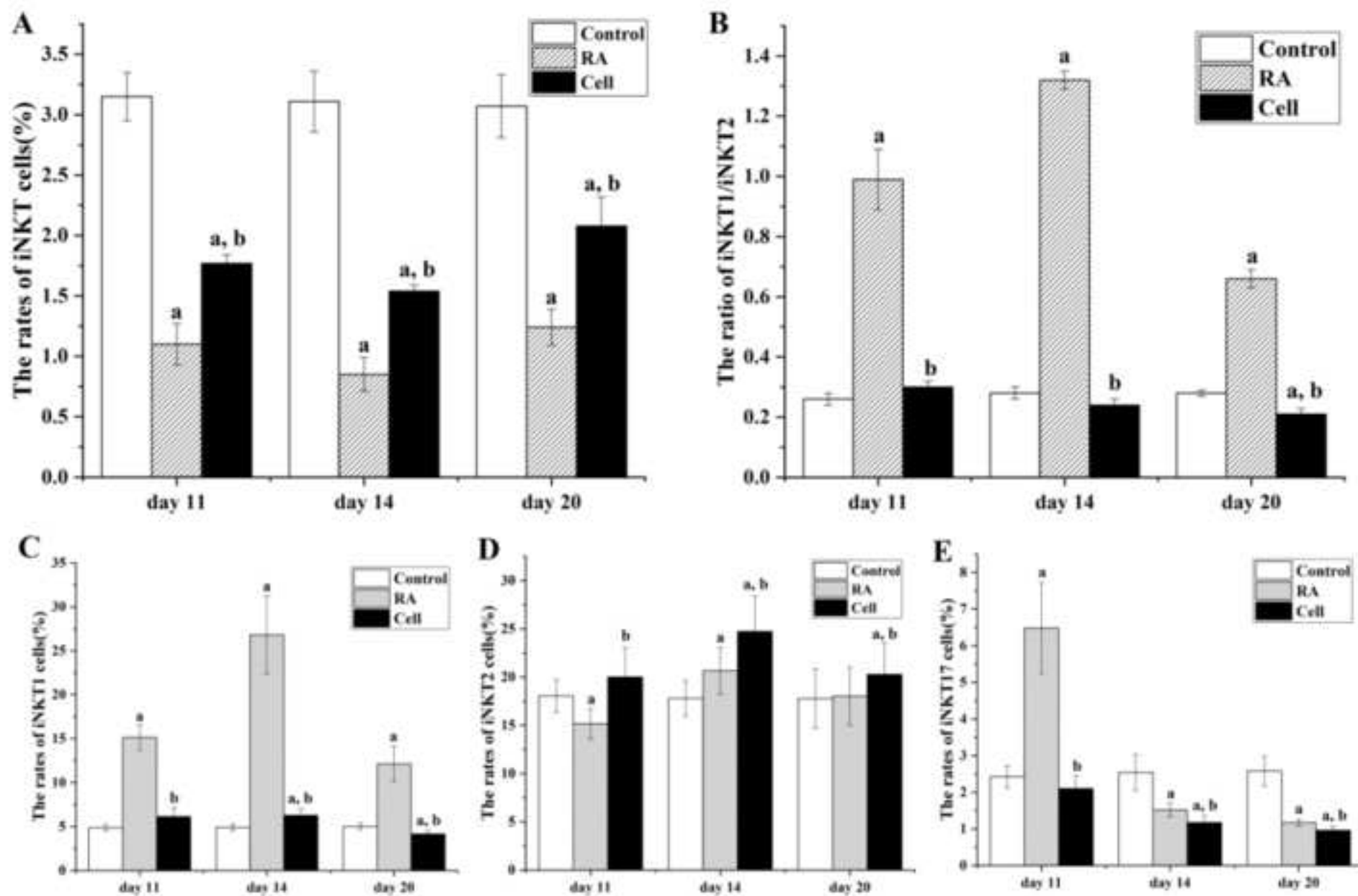624   (2019).

control   RA (day 14)   cell
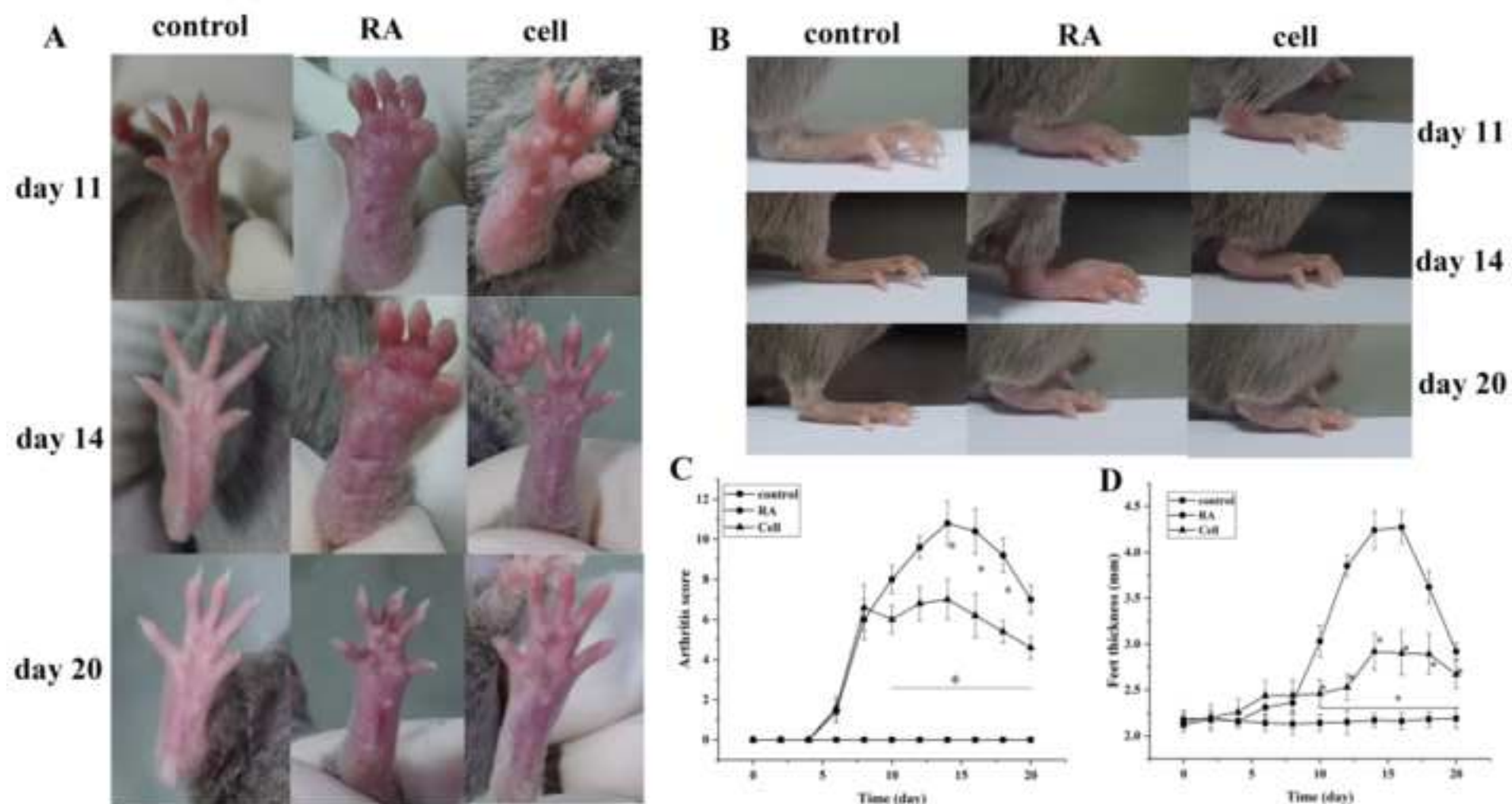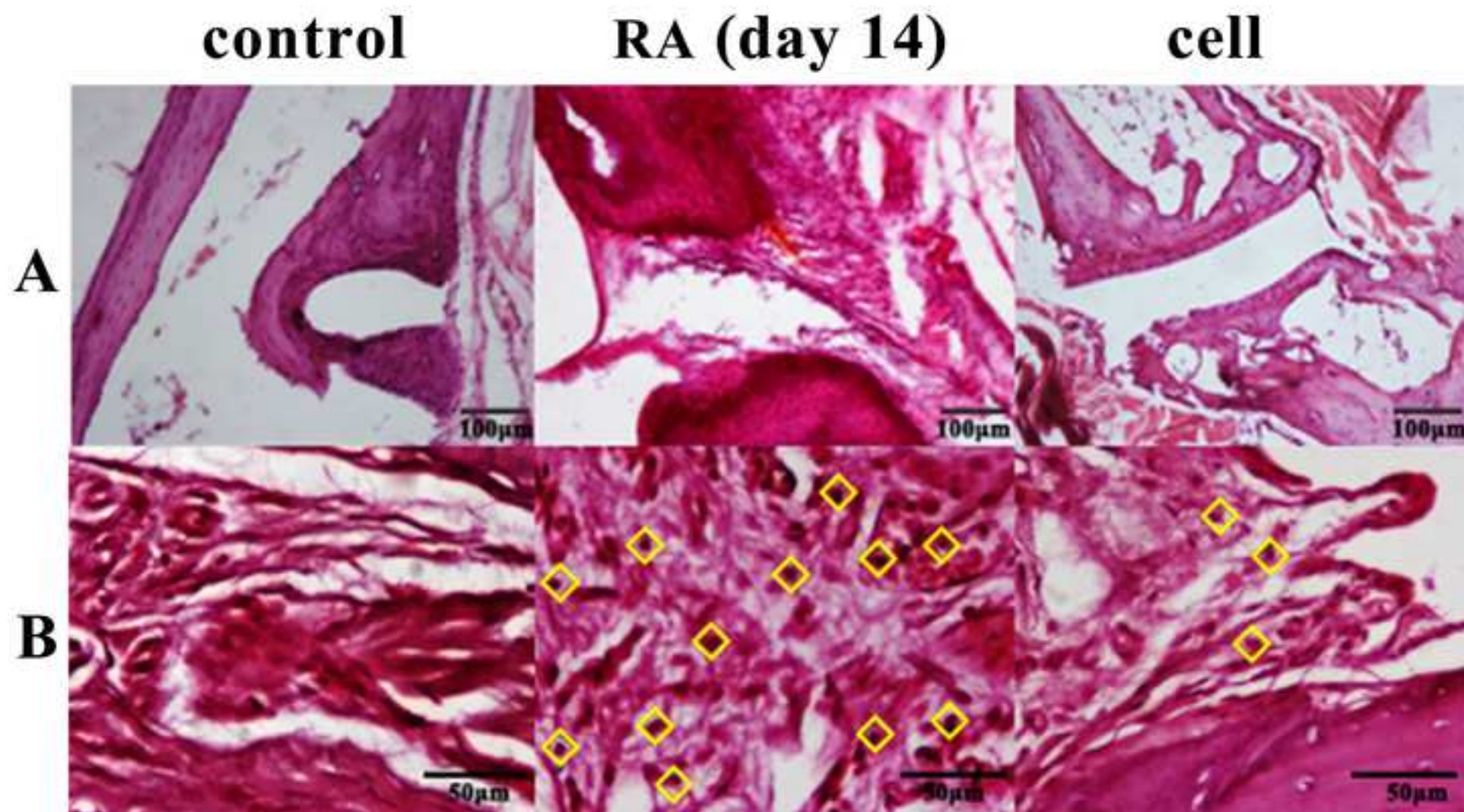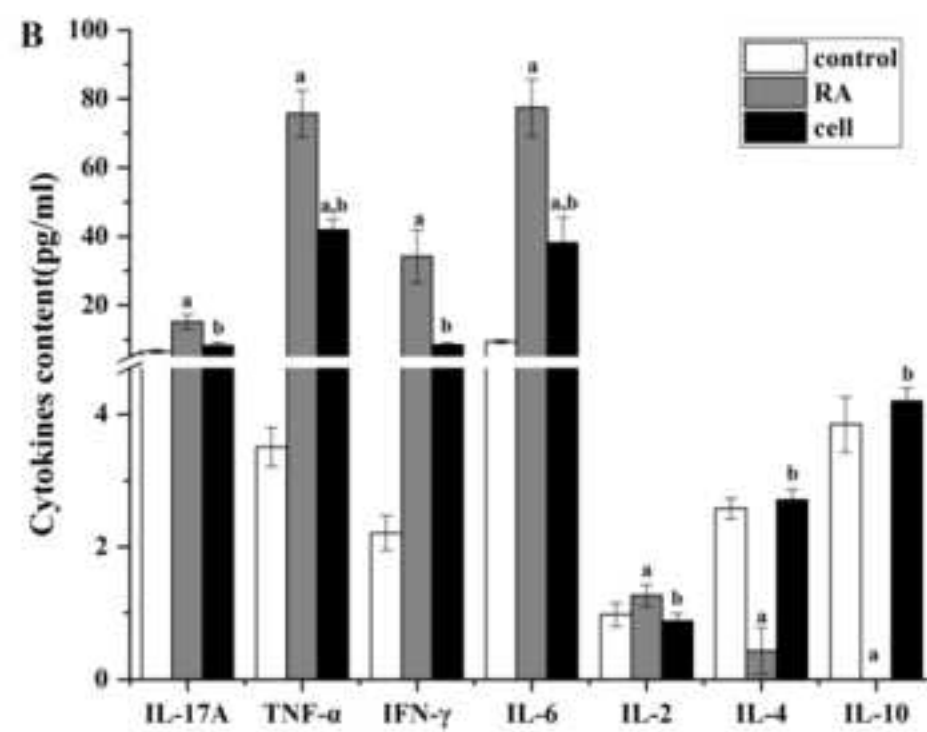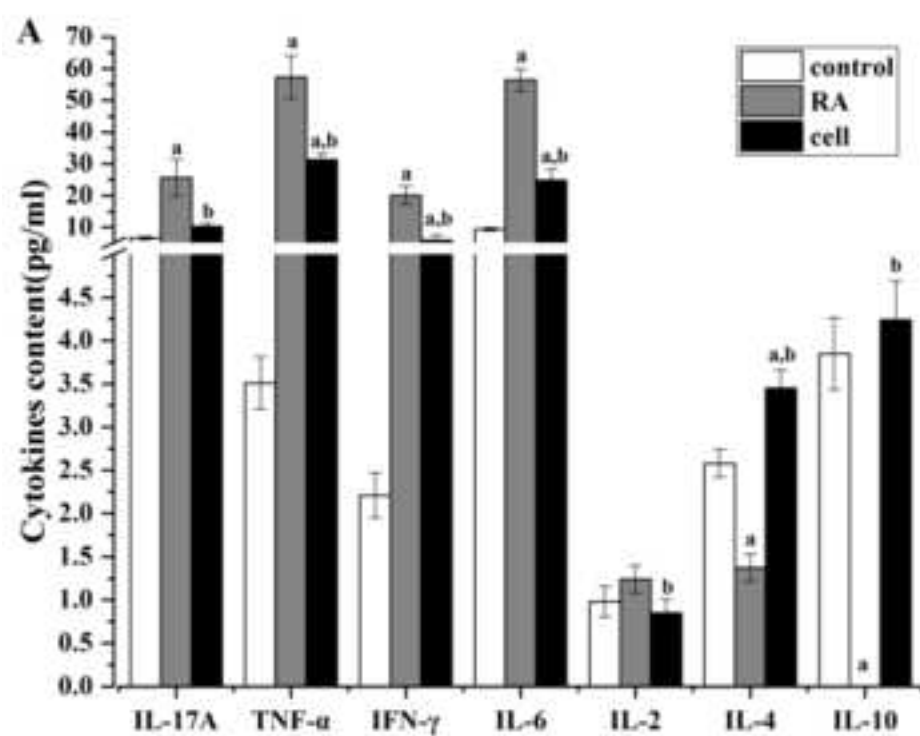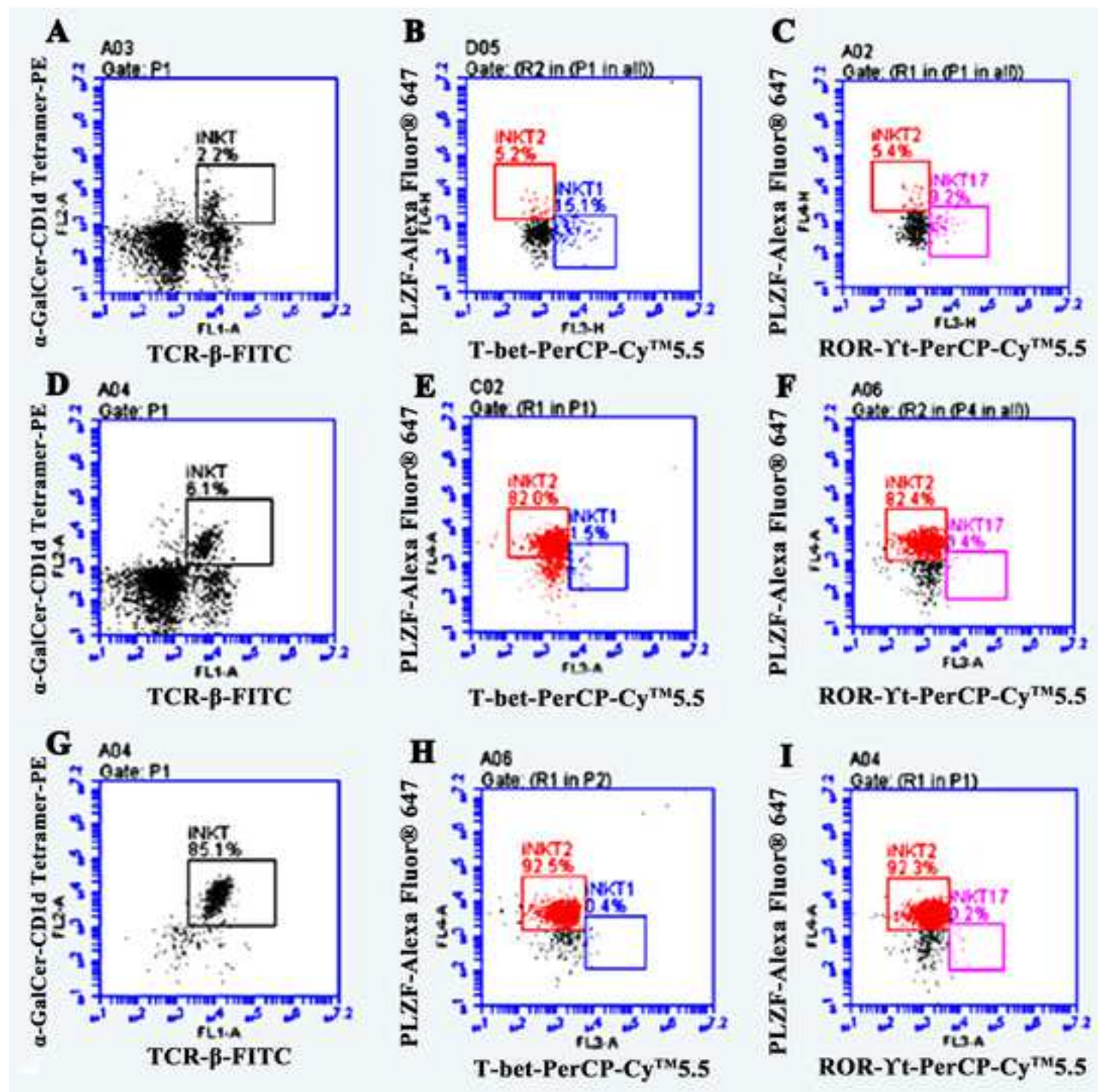
Name of Material/ Equipment	Company
Alexa Fluor 647 Mouse Anti-PLZF	BD
Anti-PE MicroBeads	Miltenyi
Columns	Miltenyi
Cryogenic Centrifuge	Beckman
DiR	Thermo Fisher Scientific
Embedding Center	Tianjin Aviation Electromechanical
FITC Hamster Anti-Mouse TCR β Chain	BD
Flow cytometer	BD
Freund's complete adjuvant	Sigma
hGPI325-339 （IWYINCFGCETH/	Karebay Biochem
hGPI469–483 （EGNRPTNSIVFTI	Karebay Biochem
In Vivo Imaging System	PerkinElmer
Ionomycin Calcium	Cayman
KRN7000	AdipoGen
Mouse CD1d Tetramer-PE	MBL
Mouse percoll	Solarbio
Optical Microscope	Olympus
PerCP-CyTM5.5 Mouse anti-ROR-Υt	BD
PerCP-CyTM5.5 Mouse anti-T-bet	BD
Pertussis toxin	Sigma
phorbol esters	Cayman

Red Blood Cell Lysis Buffer	BD
RPMI-1640	Biological Industries
Th1/Th2/Th17 cytokines kit	BD
Ultramicrotome	Leica

Catalog Number	Comments/Description
563490	America
130-048-801	Germany
MS	Germany
Allegra® X-15R	America
D12731	America
BMJ-1	China
553170	America
Accuri C6	America
F5881	America
18062202	China
18062203	China
caliper IVIS lumina II	America
10004974	America
AG-CN2-0013	America
TS-MCD-1	Japan
P8620	China
Olympus-II	Japan
562683	America
561316	America
P7208	America
10008014	America

555899	America
01-100-1ACS	Israel
560485	America
Leica EM UC6	Germany

Dear Dr. Nam Nguyen,

Thank you very much for your letter comments on the manuscript that named "Adoptive immunotherapy of iNKT cells in glucose-6-phosphate isomerase (G6PI) - induced RA mice". We appreciate the valuable and helpful comments. We have provided point-by point responses to all comments and modified accordingly the manuscript. We have also additionally improved the language of the manuscript. We uploaded the revised manuscript in the submission system, including the clear version and the markup version, and responded to and modified your comments in the markup version. Thank you again.

Kind regards,

Dongzhi Chen, Ph.D., M.D.

Department of Immunology, School of Medicine, Hebei University, No. 342, East Yuhua Road, Baoding, Hebei province, P. R China.

E-mail: chenddzz@163.com.

jove
JOURNAL OF
VISUALIZED EXPERIMENTS

1 Alewife Center #200
Cambridge, MA 02140
tel. 617.945.9051
www.jove.com

ARTICLE AND VIDEO LICENSE AGREEMENT

Title of Article:	Experimental study of adoptive immunotherapy of iNKT cells with glucose-6-phosphate isomerase (GPI)-induced RA mice
Author(s):	Ming Meng, Huifang Liu, Shengde Chen, Yuanyuan Wang, Haiyang Dou, Wenjuan Li, Dongzhi Chen

Item 1: The Author elects to have the Materials be made available (as described at http://www.jove.com/publish) via:

[√] Standard Access   [ ] Open Access

Item 2: Please select one of the following items:

[√] The Author is **NOT** a United States government employee.

[ ] The Author is a United States government employee and the Materials were prepared in the course of his or her duties as a United States government employee.

[ ] The Author is a United States government employee but the Materials were NOT prepared in the course of his or her duties as a United States government employee.

ARTICLE AND VIDEO LICENSE AGREEMENT

1.   **Defined Terms.** As used in this Article and Video License Agreement, the following terms shall have the following meanings: "**Agreement**" means this Article and Video License Agreement; "**Article**" means the article specified on the last page of this Agreement, including any associated materials such as texts, figures, tables, artwork, abstracts, or summaries contained therein; "**Author**" means the author who is a signatory to this Agreement; "**Collective Work**" means a work, such as a periodical issue, anthology or encyclopedia, in which the Materials in their entirety in unmodified form, along with a number of other contributions, constituting separate and independent works in themselves, are assembled into a collective whole; "**CRC License**" means the Creative Commons Attribution-Non Commercial-No Derivs 3.0 Unported Agreement, the terms and conditions of which can be found at: http://creativecommons.org/licenses/by-nc-nd/3.0/legalcode; "**Derivative Work**" means a work based upon the Materials or upon the Materials and other pre-existing works, such as a translation, musical arrangement, dramatization, fictionalization, motion picture version, sound recording, art reproduction, abridgment, condensation, or any other form in which the Materials may be recast, transformed, or adapted; "**Institution**" means the institution, listed on the last page of this Agreement, by which the Author was employed at the time of the creation of the Materials; "**JoVE**" means MyJove Corporation, a Massachusetts corporation and the publisher of The Journal of Visualized Experiments; "**Materials**" means the Article and / or the Video; "**Parties**" means the Author and JoVE; "**Video**" means any video(s) made by the Author, alone or in conjunction with any other parties, or by JoVE or its affiliates or agents, individually or in collaboration with the Author or any other parties, incorporating all or any portion of the Article, and in which the Author may or may not appear.

2.   **Background.** The Author, who is the author of the Article, in order to ensure the dissemination and protection of the Article, desires to have the JoVE publish the Article and create and transmit videos based on the Article. In furtherance of such goals, the Parties desire to memorialize in this Agreement the respective rights of each Party in and to the Article and the Video.

3.   **Grant of Rights in Article.** In consideration of JoVE agreeing to publish the Article, the Author hereby grants to JoVE, subject to **Sections 4** and **7** below, the exclusive, royalty-free, perpetual (for the full term of copyright in the Article, including any extensions thereto) license (a) to publish, reproduce, distribute, display and store the Article in all forms, formats and media whether now known or hereafter developed (including without limitation in print, digital and electronic form) throughout the world, (b) to translate the Article into other languages, create adaptations, summaries or extracts of the Article or other Derivative Works (including, without limitation, the Video) or Collective Works based on all or any portion of the Article and exercise all of the rights set forth in (a) above in such translations, adaptations, summaries, extracts, Derivative Works or Collective Works and (c) to license others to do any or all of the above. The foregoing rights may be exercised in all media and formats, whether now known or hereafter devised, and include the right to make such modifications as are technically necessary to exercise the rights in other media and formats. If the "Open Access" box has been checked in **Item 1** above, JoVE and the Author hereby grant to the public all such rights in the Article as provided in, but subject to all limitations and requirements set forth in, the CRC License.

jove
JOURNAL OF VISUALIZED EXPERIMENTS

1 Alewife Center #200
Cambridge, MA 02140
tel. 617.945.9051
www.jove.com

ARTICLE AND VIDEO LICENSE AGREEMENT

4. Retention of Rights in Article. Notwithstanding the exclusive license granted to JoVE in **Section 3** above, the Author shall, with respect to the Article, retain the non-exclusive right to use all or part of the Article for the non-commercial purpose of giving lectures, presentations or teaching classes, and to post a copy of the Article on the Institution's website or the Author's personal website, in each case provided that a link to the Article on the JoVE website is provided and notice of JoVE's copyright in the Article is included. All non-copyright intellectual property rights in and to the Article, such as patent rights, shall remain with the Author.

5. Grant of Rights in Video – Standard Access. This **Section 5** applies if the "Standard Access" box has been checked in **Item 1** above or if no box has been checked in **Item 1** above. In consideration of JoVE agreeing to produce, display or otherwise assist with the Video, the Author hereby acknowledges and agrees that, Subject to **Section 7** below, JoVE is and shall be the sole and exclusive owner of all rights of any nature, including, without limitation, all copyrights, in and to the Video. To the extent that, by law, the Author is deemed, now or at any time in the future, to have any rights of any nature in or to the Video, the Author hereby disclaims all such rights and transfers all such rights to JoVE.

6. Grant of Rights in Video – Open Access. This **Section 6** applies only if the "Open Access" box has been checked in **Item 1** above. In consideration of JoVE agreeing to produce, display or otherwise assist with the Video, the Author hereby grants to JoVE, subject to **Section 7** below, the exclusive, royalty-free, perpetual (for the full term of copyright in the Article, including any extensions thereto) license (a) to publish, reproduce, distribute, display and store the Video in all forms, formats and media whether now known or hereafter developed (including without limitation in print, digital and electronic form) throughout the world, (b) to translate the Video into other languages, create adaptations, summaries or extracts of the Video or other Derivative Works or Collective Works based on all or any portion of the Video and exercise all of the rights set forth in (a) above in such translations, adaptations, summaries, extracts, Derivative Works or Collective Works and (c) to license others to do any or all of the above. The foregoing rights may be exercised in all media and formats, whether now known or hereafter devised, and include the right to make such modifications as are technically necessary to exercise the rights in other media and formats. For any Video to which this **Section 6** is applicable, JoVE and the Author hereby grant to the public all such rights in the Video as provided in, but subject to all limitations and requirements set forth in, the CRC License.

7. Government Employees. If the Author is a United States government employee and the Article was prepared in the course of his or her duties as a United States government employee, as indicated in **Item 2** above, and any of the licenses or grants granted by the Author hereunder exceed the scope of the 17 U.S.C. 403, then the rights granted hereunder shall be limited to the maximum rights permitted under such statute. In such case, all provisions contained herein that are not in conflict with such statute shall remain in full force and effect, and all provisions contained herein that do so conflict shall be deemed to be amended so as to provide to JoVE the maximum rights permissible within such statute.

8. Protection of the Work. The Author(s) authorize JoVE to take steps in the Author(s) name and on their behalf if JoVE believes some third party could be infringing or might infringe the copyright of either the Author's Article and/or Video.

9. Likeness, Privacy, Personality. The Author hereby grants JoVE the right to use the Author's name, voice, likeness, picture, photograph, image, biography and performance in any way, commercial or otherwise, in connection with the Materials and the sale, promotion and distribution thereof. The Author hereby waives any and all rights he or she may have, relating to his or her appearance in the Video or otherwise relating to the Materials, under all applicable privacy, likeness, personality or similar laws.

10. Author Warranties. The Author represents and warrants that the Article is original, that it has not been published, that the copyright interest is owned by the Author (or, if more than one author is listed at the beginning of this Agreement, by such authors collectively) and has not been assigned, licensed, or otherwise transferred to any other party. The Author represents and warrants that the author(s) listed at the top of this Agreement are the only authors of the Materials. If more than one author is listed at the top of this Agreement and if any such author has not entered into a separate Article and Video License Agreement with JoVE relating to the Materials, the Author represents and warrants that the Author has been authorized by each of the other such authors to execute this Agreement on his or her behalf and to bind him or her with respect to the terms of this Agreement as if each of them had been a party hereto as an Author. The Author warrants that the use, reproduction, distribution, public or private performance or display, and/or modification of all or any portion of the Materials does not and will not violate, infringe and/or misappropriate the patent, trademark, intellectual property or other rights of any third party. The Author represents and warrants that it has and will continue to comply with all government, institutional and other regulations, including, without limitation all institutional, laboratory, hospital, ethical, human and animal treatment, privacy, and all other rules, regulations, laws, procedures or guidelines, applicable to the Materials, and that all research involving human and animal subjects has been approved by the Author's relevant institutional review board.

11. JoVE Discretion. If the Author requests the assistance of JoVE in producing the Video in the Author's facility, the Author shall ensure that the presence of JoVE employees, agents or independent contractors is in accordance with the relevant regulations of the Author's institution. If more than one author is listed at the beginning of this Agreement, JoVE may, in its sole

jove
1 Alewife Center #200
Cambridge, MA 02140
tel. 617.945.9051
www.jove.com

ARTICLE AND VIDEO LICENSE AGREEMENT

discretion, elect not take any action with respect to the Article until such time as it has received complete, executed Article and Video License Agreements from each such author. JoVE reserves the right, in its absolute and sole discretion and without giving any reason therefore, to accept or decline any work submitted to JoVE. JoVE and its employees, agents and independent contractors shall have full, unfettered access to the facilities of the Author or of the Author's institution as necessary to make the Video, whether actually published or not. JoVE has sole discretion as to the method of making and publishing the Materials, including, without limitation, to all decisions regarding editing, lighting, filming, timing of publication, if any, length, quality, content and the like.

12.   **Indemnification.** The Author agrees to indemnify JoVE and/or its successors and assigns from and against any and all claims, costs, and expenses, including attorney's fees, arising out of any breach of any warranty or other representations contained herein. The Author further agrees to indemnify and hold harmless JoVE from and against any and all claims, costs, and expenses, including attorney's fees, resulting from the breach by the Author of any representation or warranty contained herein or from allegations or instances of violation of intellectual property rights, damage to the Author's or the Author's institution's facilities, fraud, libel, defamation, research, equipment, experiments, property damage, personal injury, violations of institutional, laboratory, hospital, ethical, human and animal treatment, privacy or other rules, regulations, laws, procedures or guidelines, liabilities and other losses or damages related in any way to the submission of work to JoVE, making of videos by JoVE, or publication in JoVE or elsewhere by JoVE. The Author shall be responsible for, and shall hold JoVE harmless from, damages caused by lack of sterilization, lack of cleanliness or by contamination due to
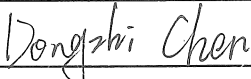
the making of a video by JoVE its employees, agents or independent contractors. All sterilization, cleanliness or decontamination procedures shall be solely the responsibility of the Author and shall be undertaken at the Author's expense. All indemnifications provided herein shall include JoVE's attorney's fees and costs related to said losses or damages. Such indemnification and holding harmless shall include such losses or damages incurred by, or in connection with, acts or omissions of JoVE, its employees, agents or independent contractors.

13.   **Fees.** To cover the cost incurred for publication, JoVE must receive payment before production and publication the Materials. Payment is due in 21 days of invoice. Should the Materials not be published due to an editorial or production decision, these funds will be returned to the Author. Withdrawal by the Author of any submitted Materials after final peer review approval will result in a US$1,200 fee to cover pre-production expenses incurred by JoVE. If payment is not received by the completion of filming, production and publication of the Materials will be suspended until payment is received.

14.   **Transfer, Governing Law.** This Agreement may be assigned by JoVE and shall inure to the benefits of any of JoVE's successors and assignees. This Agreement shall be governed and construed by the internal laws of the Commonwealth of Massachusetts without giving effect to any conflict of law provision thereunder. This Agreement may be executed in counterparts, each of which shall be deemed an original, but all of which together shall be deemed to me one and the same agreement. A signed copy of this Agreement delivered by facsimile, e-mail or other means of electronic transmission shall be deemed to have the same legal effect as delivery of an original signed copy of this Agreement.

A signed copy of this document must be sent with all new submissions. Only one Agreement is required per submission.

CORRESPONDING AUTHOR

Name: | Dongzhi Chen

Department: | Medical College

Institution: | Hebei University

Title: | Experimental study of adoptive immunotherapy of iNKT cells with glucose-6-phosphate isomerase (GPI)-induced RA mice

Signature: | *Dongzhi Chen*   Date: | 20-5-2019

Please submit a **signed** and **dated** copy of this license by one of the following three methods:
1. Upload an electronic version on the JoVE submission site
2. Fax the document to +1.866.381.2236
3. Mail the document to JoVE / Attn: JoVE Editorial / 1 Alewife Center #200 / Cambridge, MA 02140